A lesson in preparedness: Assessing the effectiveness of low-cost post-wildfire flood protection measures for the catastrophic flood in Kineta, Greece

George Papaioannou[1], Angelos Alamanos[2], Mohammed Basheer[3], Nikolaos Nagkoulis[4], Vassiliki Markogianni[5], George Varlas[5], Angelos Plataniotis[6,7], Anastasios Papadopoulos[5], Elias Dimitriou[5] and Phoebe Koundouri[4,7,8]

[1] Department of Forestry and Management of the Environment and Natural Resources, Democritus University of Thrace, 68200 Orestiada, Greece
[2] Independent Researcher, Berlin, 10243, Germany
[3] Department of Civil & Mineral Engineering, University of Toronto, Toronto, Ontario, Canada
[4] School of Economics and ReSEES Research Laboratory, Athens University of Economics and Business, Athens 10434, Greece
[5] Hellenic Centre for Marine Research, Institute of Marine Biological Resources and Inland Waters, Anavissos, 19013 Attiki, Greece
[6] National and Kapodistrian University of Athens, Athens, Greece
[7] UN SDSN (Global Climate Hub, European Hub, Greek Hub), Athens, Greece
[8] Department of Technology, Management and Economics, Denmark Technical University (DTU), Kongens Lyngby 2800, Denmark

Correspondence to: George Papaioannou (gpapaio@fmenr.duth.gr)

Abstract. Climate change–driven wildfires, especially in the Mediterranean, are not only becoming more frequent and severe but also amplifying flood risks by altering catchment hydrology. Yet, post-fire flood risk management remains inadequately addressed. In response, we develop an integrated simulation framework that combines meteorological, hydrological, hydraulic-hydrodynamic models and remote sensing techniques to represent post-wildfire flood hazards and support the design of Post-wildfire Flood Protection Treatments (PFPTs). We utilize the framework to accurately represent a post-wildfire flash flood event in a Mediterranean catchment in Greece. The flood event is simulated under three scenarios: pre-wildfire, post-wildfire without any PFPTs in place (reality), and post-wildfire with PFPTs. The results show that the wildfire's impact on flood extent was around a 24.1% increase, but the PFPTs could have counterbalanced this impact. Moreover, we present an economic model for estimating the cost of the recommended PFPTs and the flood damage direct costs, combining an accounting and a semi-automated AI-based approach. The cost comparison reveals that the protection would have cost around €5.05mill (just the 20% of the flood damage costs, €25.2mill) potentially saving €6.37mill in flood damage. By filling critical knowledge gaps, our study offers insights into the dynamics of post-wildfire flood events and provides policymakers with valuable insights for timely risk mitigation amidst escalating fire-related disasters.

Keywords: Wildfires; Flood protection; Barrier treatments; In-channel treatments; Hydraulic modelling; Rain-on-Grid; Meteorological modelling; Remote Sensing; Protection Cost.

1 Introduction

The escalating frequency and intensity of wildfires, attributed to climate change, present an unprecedented challenge with widespread and complex ramifications for both ecosystems and human populations (Wang et al., 2020). Although wildfires are most prevalent during summer periods, the associated damages persist longer, posing severe risks (Brogan et al., 2019b, a). Wildfires can cause substantial alterations in vegetation, soil conditions, land cover, hydromorphology, and the hydrological response of burned catchments during storm events (Alamanos, 2024; Hasan et al., 2020). The implications become apparent when the first extreme storms occur, and the burned sites are found to be more vulnerable to flash floods due to their reduced infiltration capacity, sensitivity to peak flows, and increased runoff and sediment transport loads (Havel et al., 2018). The Mediterranean region, a climate change hotspot, has been particularly vulnerable to increasingly severe wildfires and flood events over the last few years, and such threats are anticipated to become more prevalent in the future (Cos et al., 2022). Thus, it is imperative to better understand the dynamics of such risks and to be proactive through continuous resilience-building efforts. A better understanding of fire-flood dynamics and their effects can be achieved through data-driven models, which explore the flooding response in burned sites. Resilience-building efforts after a wildfire involve, at a minimum, treatments to protect the burned sites from extreme runoff and soil erosion. The cost and effectiveness of these approaches for enhancing preparedness for flood hazards are scrutinized in this paper.

Data-driven approaches for evaluating the flood impacts of wildfires include hydrological simulations of post-wildfire runoff and flood mapping of burned sites. The former is more common and focuses on how wildfires change soil and hydrological properties, how they recover, or even perform experiments to quantify the differences in hydrological responses (Ebel and Martin, 2017). The latter includes only a few applications in the literature, as such models are data-intensive. Typically, these models simulate various storms, aiming to present different risk scenarios. Theochari and Baltas (2022) analyzed the hydrological and hydraulic responses of flood-prone areas in a burned site on Evia Island, Greece, to a design storm. Godara et al. (2023) applied the hydraulic model Telemac to investigate how a Norwegian catchment responds to a design flood. Chrysovergis et al. (2021) studied a real post-wildfire event that caused flood and erosion damages in Southern California, with the focus being on the factors that caused the damages. These studies indicate that burned areas are more vulnerable to flash floods due to increased soil imperviousness and peak discharge, underscoring the necessity for accurate models for flood inundation mapping and assessing post-wildfire protection measures. However, such studies are very scarce in the literature.

Post-wildfire Flood Protection Treatments (PFPTs) aim to protect burned areas from flooding and other hazards, such as landslides and soil erosion, which are linked to extreme precipitation (Basheer and Oommen, 2024). PFPTs include several interventions that are case-specific, depending on the site's physical characteristics. PFPTs include barriers, mulch or

hydromulch, and seeding (aiming for a quicker recovery of the burned area), silt fences, erosion control mats, or the installation of in-channel structures (e.g., trees, log-erosion barriers, check dams) to 'cut' excess runoff and debris flows. The main and most common PFPT types, according to Napper (2006) and Papaioannou et al. (2023), are the land treatments (installing barriers to reduce runoff and erosion), and channel treatments (in-stream interventions for water control). Barrier-based land treatments are more suitable for areas with high to moderate burn severity and slopes of up to 60%. Channel treatments, on the other hand, are most suitable in small headwater channels, typically where soil burn severity is moderate to high, altered hydrologic response elevate the risk to downstream values and channel gradients are gentle enough for stable installation, ensuring site accessibility for timely maintenance and inspection. There is a lack of studies on the performance of PFPTs, with the majority of the studied cases being in the US, Spain and Portugal (Girona-García et al., 2021). While there are some studies on the application of PFPTs, these primarily refer to specific types of measures, mostly focusing on soil erosion rather than flood hazards, and are highly case-specific (Girona-García et al., 2023; Robinne et al., 2020). In one of the few examples evaluating the effectiveness of PFPTs, Kastridis and Kamperidou (2015) focus on two northern Greek basins, where the applied measures included cutting burned trees, a total ban on grazing, and the construction of log erosion barriers, log check-dams, and contour branch barriers. They observed failures of these PFPTs, mainly due to the rush of construction and their poor implementation, which resulted in subsequent floods. The importance of the timely and properly planned installation of PFPTs to enhance their effectiveness in mitigating post-wildfire flood risks is also highlighted by Theofanidis et al. (2025) and Mitsopoulos et al. (2022), studying another Greek burned site. A similar study (Posner and Georgakakos, 2017) evaluated the feasibility and impact of check-dams (gabion-dams) and vegetation coverage PFPTs in the mountainous areas of Haiti, indicating that hillslope revegetation primarily impacts lower return period storms, while channel vegetation reduces peak discharge and delays flood peaks, and combined gabion dams and channel vegetation effects are non-linear and dependent on storm characteristics. But, to the best of our knowledge, no study simulates a real post-wildfire flood event along with suitable PFPTs to test the effects of the fire and the role of PFPTs in the actual flooding. Even more scarce in the academic literature are studies evaluating the PFPT costs, considering various components from installation to material and labour costs, probably due to the case- and context-specific nature of this problem. These costs are often cited as the greatest obstacle to their implementation.

Reflecting on the above, there are three apparent research gaps. First, there are very few studies on the response of burned sites to real flood events, as simulated by hydraulic models. Second, the role of PFPTs remains under-explored, and despite some general (national) guidelines for the selection and installation of certain treatments, there is still room for improvement in simulating and assessing their effectiveness and associated economic implications (Papaioannou et al., 2023). Third, the costs associated with applying the necessary PFPTs, and especially their comparison with the flood damage costs that can occur, are a crucial analysis to reveal whether and how beneficial the PFPTs can be for building flood resilience. In this paper, we aim to cover these three gaps by: i) a detailed representation of a post-wildfire flood event in a typical Mediterranean site, based on our previous works combining atmospheric model with remote sensing and hydraulic modelling (Alamanos et al., 2024b; Varlas et al., 2024). ii) Assessing the most appropriate PFPTs and modelling them spatially. iii) Assessing their effectiveness

for flood mitigation, by directly incorporating in the hydraulic model. iv) Estimating their costs, as well as comparing them with the estimated direct flood damage costs. Each one of these analyses, and especially their combination, is a novel contribution with direct practical and policy insights to address the increasing threat of post-wildfire flood effects, both in terms of understanding and mitigation.

2 Study area and post-wildfire flood event

A Mediterranean catchment was selected as the application area: Kineta catchment in western Attica, central Greece (Fig.1). It covers approximately 40 km^2. Its northern part is mountainous and gradually lowers to the southern part, where the coastal town of Kineta is located. The climate of the Kineta catchment, like most Mediterranean areas, has hot, dry summers and mild, wet winters (Kourgialas, 2021). The main land uses are forests (pine forests in the north, which were the main burned areas), complex cultivation patterns with various fields in the southern part, and urban settlements (the coastal Kineta town). The broader region has faced increasing wildfire risks over the past few years, with notable events in the summers of 2017 and 2018. These wildfires consumed the mountainous pine forest, a few houses in Kineta town and two smaller settlements, also causing several injuries. Following the 2018 wildfire, protection measures primarily focused on safeguarding the road network against landslides (Lekkas et al., 2019). An extreme storm event on November 24-26, 2019, led to a flash flood that caused severe damage to the town of Kineta. The wildfire contributed to this flood event, as the forest and vegetation conditions had not sufficiently recovered from the 2018 wildfire. Prior to the storm that caused the flood, the streams were blocked by sediments accumulated since the wildfire (Lekkas et al., 2019).

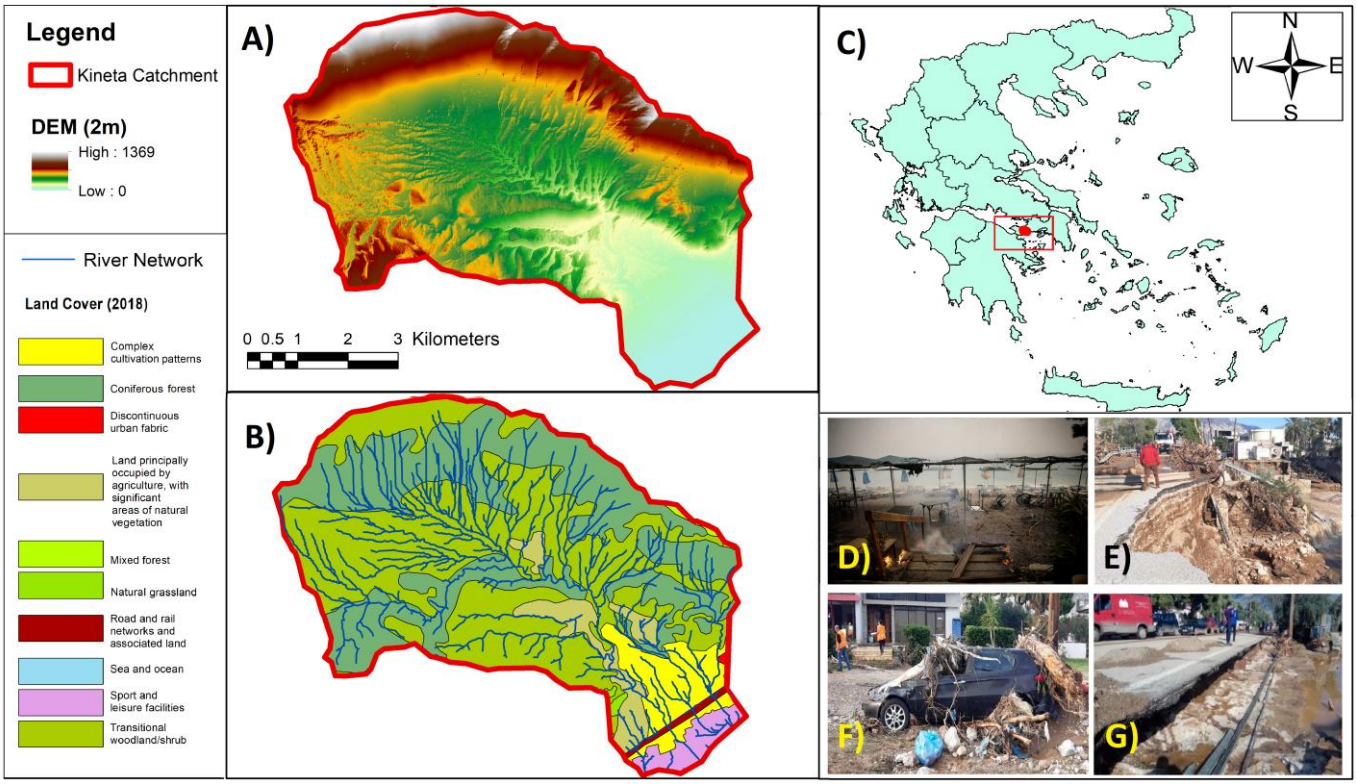

Figure 1: A) The Kineta catchment's digital elevation model (DEM). Adapted from: National Cadastre and Mapping Agency S.A. (NCMA, 2021) B) The main land cover types and the river network. C) Kineta's location in Greece (red dot). D) A picture from the wildfire of 2018, which initiated from the mountainous part of the catchment and reached the coast. F-G) Damages caused by the flood of 2019, affecting critical infrastructure and properties. Sources: (Lekkas et al., 2019; Protothema, 2019).

2 Materials and Methods

The framework consists of the following steps (Fig.2): First, we simulate the storm that caused the studied flood event (atmospheric model). Second, Remote Sensing (RS) techniques were used to identify the flooded area (flood extent) and determine the burn extent and severity, which are crucial factors in assessing the wildfire's impact on the flood through altered roughness coefficients. Next, we used a hydraulic model to simulate the flood event (RS-validated). We then designed the PFPTs and modified the terrain in the hydraulic model to incorporate them, allowing us to run different scenarios to assess their effectiveness (pre-wildfire, post-wildfire, with and without PFPTs). Finally, for each scenario, we estimated the cost of the PFPTs and the direct flood damages to compare them and provide policy insights. The methodology for each step is presented below.

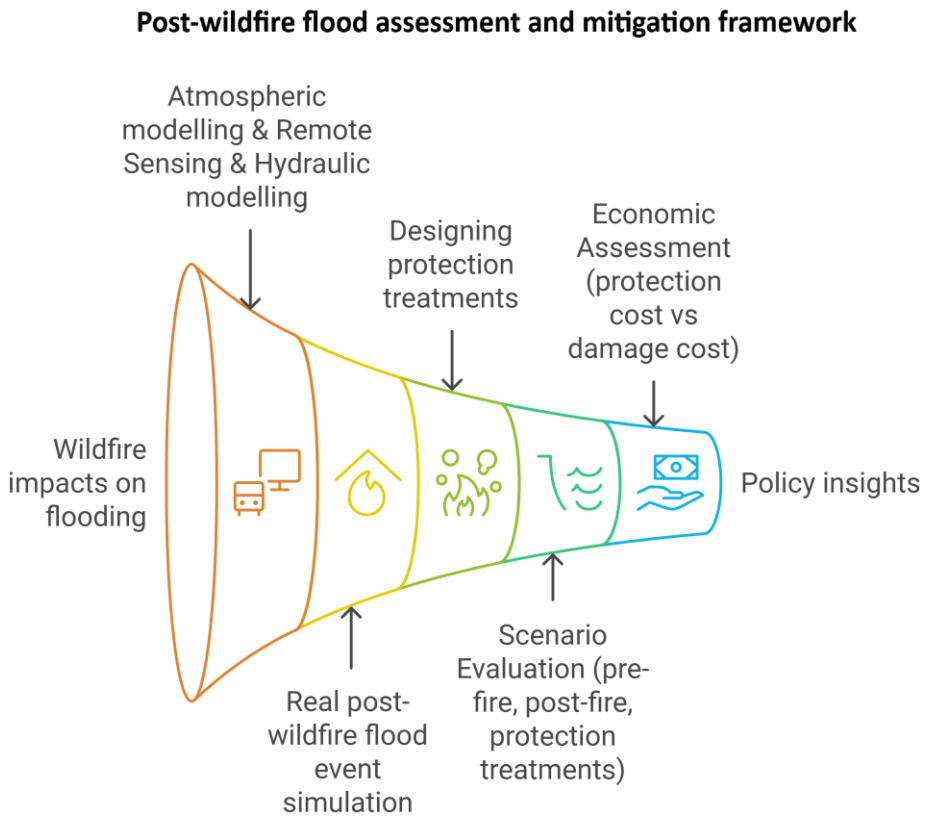

Figure 2: The general conceptual approach of the presented framework.

2.1 Atmospheric model

The storm simulation was achieved by applying the Advanced Weather and Research Forecasting (WRF-ARW) v4.2 model. The WRF-ARW atmospheric model has been successfully used in previous applications for simulating meteorological phenomena in several case studies, including those in Greece. These applications include heavy precipitation events and storms, as well as their forecasts (Alamanos et al., 2024b; Varlas et al., 2024).

The WRF-ARW model simulated the meteorological conditions that led to the storm of 24-25 November 2019, as presented in detail in Alamanos et al. (2024b). The initialization time of the simulation was set at 00:00 UTC on November 24th (02:00 local time), and the simulation lasted 48 hours until 00:00 UTC on November 26th (02:00 local time). Initial and boundary conditions were set using data from the Global Forecasting System (GFS) with a horizontal grid spacing of 0.25°×0.25°. These conditions involve atmospheric data across multiple layers, soil moisture, and temperature. Sea surface temperature (SST) for the lower boundary conditions was updated every 6 hours, utilizing the real-time global (RTG) SST analysis dataset on a grid spacing of 0.083°×0.083°. Ground processes were parameterized through the unified Noah land surface model (Tewari et al., 2004). The parameterization of the long-wave and short-wave radiation processes was based on the RRTMG scheme (Iacono

et al., 2008), while the cloud microphysics processes were parameterized by the WSM 5-class scheme (Hong et al., 2004). Convective processes were managed by the Grell-Freitas ensemble scheme for the first domain (9km×9km) and explicit convection resolution for subsequent domains (3km×3km and 1km×1km) (Grell and Freitas, 2014). Finally, the planetary boundary layer and surface layer processes were resolved by the Yonsei University scheme (YSU) and the revised Monin-Obukhov scheme, respectively (Hong et al., 2004).

2.2 Remote sensing

For the identification of the wildfire impacts and their accurate representation in the hydraulic model, we processed three Sentinel-2 MSI images (one pre-fire and two post-fire) from the Copernicus Open Access Hub. Using QGIS 3.6.3 and the semi-automatic classification plugin, we converted digital numbers to top-of-atmosphere reflectance and applied DOS1 atmospheric correction. We delineated the study area and calculated the Normalized Burn Ratio (NBR) from the NIR (B08) and SWIR (B12) bands. We then derived the change in NBR (dNBR) by subtracting the post-fire values from the July 20, 2018, reference. Applying a +0.1 dNBR threshold and USGS-recommended burn severity classes, we produced a burn severity map. By overlaying land-use data, we assigned updated Manning's n roughness coefficients to represent burned conditions in the hydraulic model, as explained below. For more details, as presented also in Alamanos et al. (2024b), see Section S1 and Fig. S1 in the Supporting Information (SI).

RS analysis was also used to obtain a picture of the actual flood extent for the November 24th event, allowing us to validate the hydraulic model. We used a single Sentinel-2 image from November 25th, 2019 (Level 1C, 09:23 UTC). After converting digital numbers to top-of-atmosphere reflectance and applying DOS1 atmospheric correction in QGIS, we evaluated five spectral water indices (NDWI, MNDWI, AWEI, RSWIR1, and RSWIR2) and transformed SWIR2, NIR, and red bands into HSV colour space. For each index, we performed histogram analysis to identify peak values (positive for water, negative or zero for land) and manually adjusted thresholds to match drone footage and post-flood imagery. Binarizing each index produced logical water masks, which were combined into a final inundation map. This observed flood polygon served as the validation dataset for our hydraulic model (validation polygon). For more details, see Section S1 and Fig.S2 in the SI.

2.3 Hydraulic - Hydrodynamic model

The flash flood was modelled within the 2D Hydrologic Engineering Center's River Analysis System (HEC-RAS) (Hydrologic Engineering Center (HEC), 2022). The input data was:

- The Digital Elevation Model (DEM) of the area, obtained by the National Cadastre and Mapping Agency S.A. (NCMA), has a 2-m resolution to achieve fine-quality and detailed simulation even at small scales, including the detailed representation of the stream network.
- The meteorological conditions were obtained from the WRF-ARW simulated precipitation. The output of WRF-ARW (section 2.1) was applied as a rain-on-grid input in HEC-RAS. The rain-on-grid technique is a relatively new approach that enables users to apply spatial datasets of gridded rainfall to the study area, in contrast to traditional point

observations (Alamanos et al., 2024b; Papaioannou et al., 2021). Therefore, 20 spatial datasets/grids were inserted into HEC-RAS, representing the storm event from November 24th, 2019, at 14:00:00 to November 25th, 2019, at 09:00:00, using a 1-hour time step.

- The Manning's roughness coefficients (n) coefficients of the catchment. The most common approach to define n is to use typical minimum, median, and maximum values from the literature for similar areas in similar conditions. We considered the land cover maps (CORINE) and their overlapping burn extent areas and burned severity classes (as estimated using RS techniques – Section 2.2) (Wu et al., 2021). For each combination of land cover-burned extent and severity, we assigned n coefficients based on the literature for both the pre-wildfire and post-wildfire conditions (Table S1). Following this process, the spatially distributed Manning's roughness coefficients were estimated. For more details, see Section S2 and Table S1 in the SI.

The model provides the flood inundation (extent), water depth and velocity for each time step of the simulated event, and the flood maximum arrival time in both pre-wildfire (hypothetically, if the same storm had occurred before the wildfire), and post-wildfire cases, for comparison purposes. The flood extent results (validation polygon) produced by the RS techniques (Section 2.2) were used to validate the results of the HEC-RAS model. The accuracy of the hydraulic model was quantified using the Critical Success Index (CSI), a widely recognized metric for flood inundation models (Zotou et al., 2022). The CSI takes into account the correctly simulated flooded areas against the validation polygon while considering the false-simulated flooded areas, as well as those areas that flooded but were not predicted by the model (Nandam and Patel, 2024). For more details, see Section S4 in the SI.

2.4 Post-wildfire Flood Protection Treatments (PFPTs) and scenarios for evaluating their effectiveness

The PFPTs would aim to protect the Kineta catchment after the 2018 wildfire from upcoming extreme storm events, including the 2019 flood. However, such measures were not fully in place or were only poorly installed.

We evaluated the most suitable PFPTs for the catchment. First, we conducted a literature review to assess all available information on PFPT types and cost-effectiveness (see Section S5 and Table S3 in the SI) (Papaioannou et al., 2023). We observed that the most commonly used PFPTs are land barriers and channel barriers, mainly due to technical practicality and lower (installation) costs. Particularly in Greece, these refer to barrier-based log-erosion barriers (LEBs) and channel-based wooden check dams (WCDs), respectively. We also reviewed the official Greek studies for PFPTs' application, which were released after the 2023 wildfires in the country, suggesting such treatments for similar case studies to the Kineta catchment (Greek Ministry of Environment and Energy, 2023; Koudoumakis et al., 2024). They also suggested LEBs and WCD due to their low cost and ease of installation using local timber, expecting that these structures can trap sediments, reduce excess flow, and slow runoff, thus protecting downstream areas from floodwaters and sediments (Alamanos et al., 2024a). Thus, we designed a series of LEBs and WCD for the Kineta catchment, tailored to its size and slopes, as follows:

- 0.2-meter high LEBs (suitable for areas with moderate to high burn severity and slopes between 10%-50%) are installed every 10m along the contour lines

- 1-meter high WCD (usually recommended for slight slopes <20%) are placed in the 1st, 2nd, and 3rd order streams at intervals of 10m, forming a continuous line of protection also at the points of intersection with the LEBs.

The designed PFPTs are shown in Fig. S3 of the SI. The resulting PFPT design forms a dense and realistic network of continuous 'protection lines' across streams and slopes.

Having designed the PFPTs spatially, we can modify the terrain of the HEC-RAS model accordingly. The terrain was modified to incorporate the suggested PFPTs according to Fig.S3 using the R package "terra" to analyze the raster file with the designed PFPTs (Fig.S3), the R package "sf" to analyze vectors (placing thus the LEBs and WCD in the defined intervals), and the R package "smoothr" for lines smoothing, making the PFPTs suggested installation realistic (see section S5 in the SI). We then run different scenarios in the HEC-RAS model:

- **Pre-wildfire, No PFPTs (wildfire effect scenario):** the same storm applies in the catchment with pre-wildfire conditions, using the respective Manning's n coefficients from Table S1. No PFPTs are in place. This hypothetical scenario was simulated for comparison purposes of the pre- and post-wildfire situations, aiming to isolate the effect of the wildfire on flooding.
- **Post-wildfire, No PFPTs (reality scenario):** the same storm applies in the catchment with post-wildfire conditions, using the respective Manning's n coefficients from Table S1. No PFPTs are in place. This is the reality of what happened in Kineta, so the results of this scenario were the ones that were validated, and all roughness coefficients were adjusted accordingly. In this scenario, the major culverts were excluded from the modelling, and the bridge geometry was modified in the DEM to represent full blockage by sediment and debris, consistent with field observations from the actual flood event.
- **Post-wildfire, With PFPTs (protection scenario):** the same storm applies in the catchment, with post-wildfire conditions, using the respective Manning's n coefficients from Table S1, and the modified terrain that includes the PFPTs, so that the designed network of LEBs and WCD is in place. This is our suggested wish-case, where protection should have been considered after the wildfire, to mitigate potential future floods. In this scenario, it was assumed that PFPT works would retain debris, and thus, major culverts and bridges would not be blocked.

The results of these scenarios were tested in terms of i) flood extent (area), ii) water depth, iii) water velocity, iv) flood maximum arrival time, and v) costs and damages (analyzed in the following sections).

2.5 Economic analysis: PFPTs cost vs Flood damage cost

From an engineering perspective, post-wildfire flood resilience heavily relies on the application of necessary protection measures. From an economic or policy perspective, however, the decision to apply the PFPTs is connected to the associated costs (Alamanos et al., 2024a). We assess the direct economic implications of the proposed PFPTs' application by estimating their total implementation cost and comparing them with the direct cost of avoided damage. Our estimations for PFPTs consider the necessary material and transportation costs, as well as the installation and labour costs. This information was obtained from the Greek guidelines, which provide detailed cost breakdowns for such works. For more information, see Table S4 in the SI.

Moreover, we present a comparison of these costs with the direct cost of avoided flood damage to provide a measure of the potential value of these protection efforts. The direct damage costs caused by the flood were estimated taking into account the damages that occur due to the physical contact of objects with the floodwater (Merz et al., 2004; Thieken et al., 2009), and are usually straightforward to estimate (Brémond et al., 2013; Zabret et al., 2018).

To assess them, we counted the affected elements by the flood by inputting the flood inundation results (flooded area) into the AI tool "Segment Anything Model" (SAM) (Kirillov et al., 2023), a widely used application for image segmentation. This tool delineates the objects in the area (e.g. houses, commercial buildings, agricultural fields). A human check-counting was also performed by navigating in Google Street Maps and comparing the results to ensure that the identified elements were complete and correctly counted (see Section S6, Fig.S4, and Table S5 in the SI). Thus, this semi-automated approach involving Artificial Intelligence (AI) provided us with accurate estimates of the affected properties. Then, typical insurance and monetary values were used to calculate the direct flood damage costs for those affected properties (see Section S6 and Table S5 in the SI). For the calculation of the economic losses due to a blocked road (Athens-Corinth highway) from flooding, we used a general estimation model (Eq. S2), which takes into account factors like the daily vehicle traffic, the additional distance of detour, vehicle operating costs, additional travel time, and the direct economic value of time and goods affected (see section S6, and Eq.S2, in the SI). Finally, the infrastructure damages were considered (repair costs of roads, streams, land, and drainage) as reported by the local authorities (see section S6, in the SI).

For all scenarios (Pre-wildfire, No PFPTs; post-wildfire, No PFPTs; and Post-wildfire, with PFPTs), flood damage costs were estimated based on the flood extent (area-based), as we only account for direct costs. The results of the "reality" scenario (Post-wildfire, No PFPTs) were validated over the official Greek estimates for restoring the damages in Kineta. For the other two hypothetical scenarios (Pre-wildfire, No PFPTs and Post-wildfire, With PFPTs), we also assume that the Athens-Corinth highway would have been blocked, and we follow an area-based approach to calculate the infrastructure costs.

3 Results

3.1 Atmospheric model results

The storm of November 24th and 25th was extreme, as a deep barometric low originating from the west led to substantial precipitation across various regions in Greece. A cold front accompanying this low-pressure system triggered heavy rainfall in Kineta and its neighbouring areas during the night of November 24th to 25th. The meteorological station of the National Observatory of Athens (NOA) network at Agioi Theodoroi (approximately 8 kilometres southwest of Kineta) recorded a total rainfall of 206.8 millimetres over the two-day period of November 24th to 25th (Meteo, 2024). The results of the WRF-ARW simulation estimated a rainfall of 182.6 millimetres over the same area, aligning closely with the actual measurements. As Fig 3 shows, most of the precipitation occurred between November 24th, 20:00 UTC (local time 22:00), and November 25th, 06:00 UTC (local time 08:00). Particularly in the early morning hours of November 25th, a severe storm centred around Kineta,

evident from the pattern and intensity of the 1-hour accumulated precipitation (Fig.3) from 03:00 to 06:00 local time. These rainfall rates led to increased runoff within the Kineta catchment, which caused the flash flood.

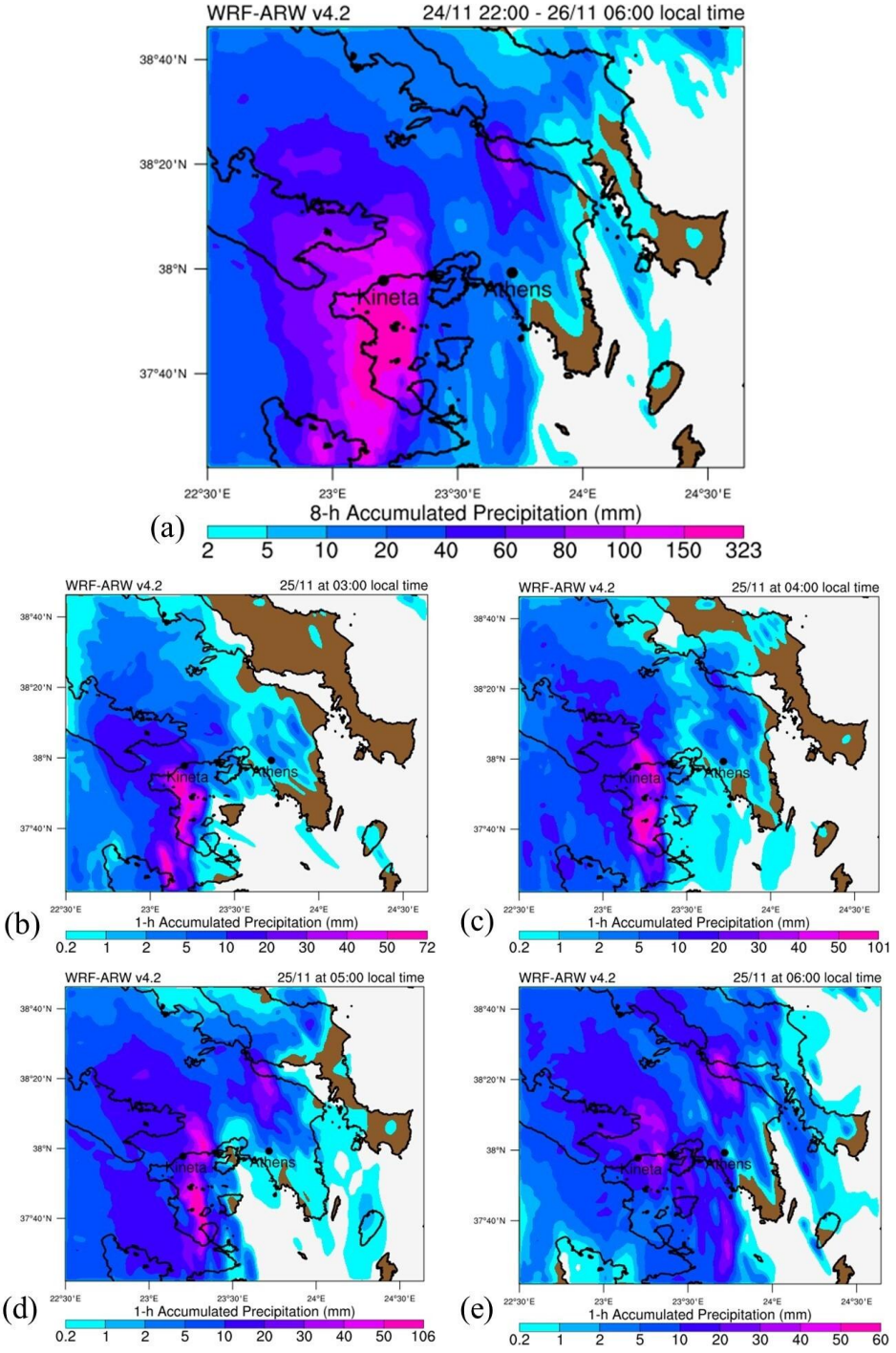

Figure 3: The results of the WRF-ARW model of the simulated accumulated precipitation (in mm) for: a) 8-h for the period from November 24th at 22:00 local time to November 25th at 06:00 local time, b) 1-h for November 25th at 03:00 local time, c) 1-h for November 25th at 04:00 local time, d) 1-h for November 25th at 05:00 local time, and e) 1-h for November 25th at 06:00 local time. Source: (Alamanos et al., 2024b).

3.2 Remote sensing results

First, the results of the RS analysis indicated the burn severity and extent, as well as their changes during the period from the wildfire until the flood event. The analysis of the dNBR revealed regrowth of vegetation after the wildfire, from August 2018 to October 2019, specifically just before the flood event. During this period, the proportion of unburned areas (24.1%) and those with low (29.3%) or low-moderate (35.5%) burn severity increased compared to August 2018, where the corresponding percentages were 19%, 15.9%, and 21%, respectively. Furthermore, the predominant burn severity classes are those subjected to moderate-high and moderate-low severity and the unburned areas for 2018, and moderate-low and low severity and unburned area for October 2019. Notably, the extent of areas affected by high burn severity (0.01%) significantly decreased in October 2019 compared to August 2018 (12.5%), with these regions largely transitioning to areas impacted by moderate-low burn severity (Fig.4a,b, and Fig.S1). Furthermore, the RS analysis provided us with a map of the flood extent. This was produced by comparing all computed Water Indices (WIs), interpreting them with expert knowledge, and visually inspecting them while aligning them with the 4 (Red)-3 (Green)-2 (Blue) natural composite of the corresponding S2 image, as described in section 2.2. The intensified analysis revealed that the Red and Short-Wave Infrared 2 Index (RSWIR2), with a threshold value of ≥ -0.1, outperformed other indices in detecting inundated areas (Fig.4a,b). This index consistently yielded the most stable results throughout our analysis (Fig.S2).

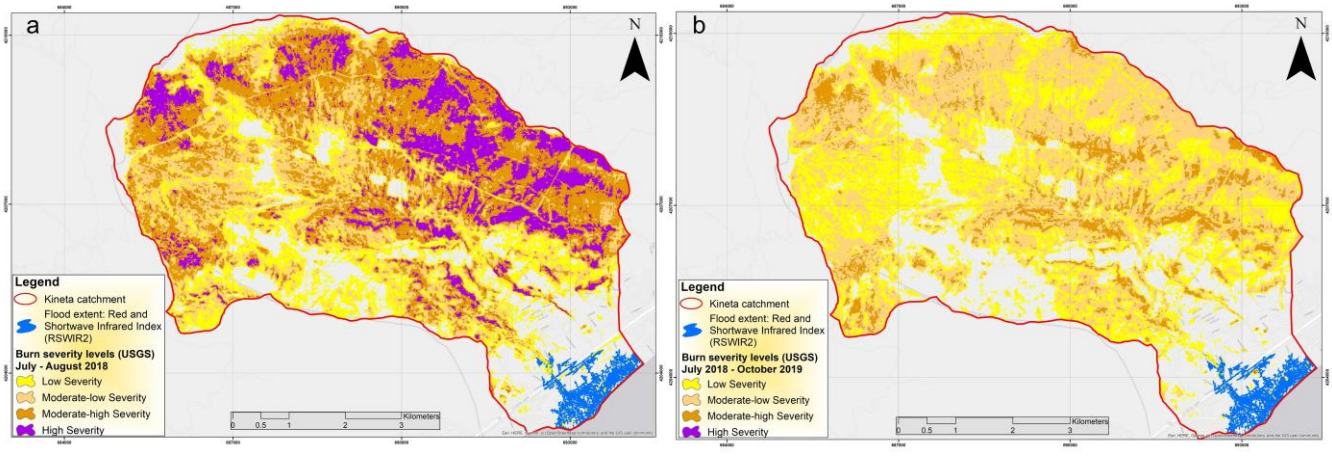

Figure 4: The RS results of the a) burn extent and severity of the wildfire period July-August 2018, b) burn extent and severity of the post-wildfire period July 2018- October 2019, both illustrating the flood extent (November 2019) according to the RSWIR2 index.

3.3 Hydraulic-hydrodynamic model results

The HEC-RAS model runs under the scenarios described in section 2.4 (pre-wildfire, post-wildfire, without and with PFPTs in place).

The model's accuracy was tested by the CSI scores, for the real case of the Post-wildfire, No PFPTs simulation, using the validation polygon. The CSI score reached 0.65, indicating satisfactory performance (CSIs above 0.5 are acceptable) (Equation S1) (Zotou et al., 2022).

The total simulated flood inundation area for the (real) post-wildfire case was 595,246 m^2, covering almost 24% of the town's total residential area. The pre-wildfire simulation resulted in a flood inundation area of 451,848 m^2. The difference in these flood extents reflects the impact of the wildfire on the flooding, which is 143,398 m^2. If the PFPTs were in place after the wildfire, the flood extent would have been 447,575m^2. Therefore, the effect of these recommended protection measures would have reduced the flood-inundated area by 147,671 m^2 (24.8%) (see detailed results in Fig. S5). It is worth noting that this difference indicates that the effect of the wildfire could have been entirely avoided with the PFPTs.

Figure 5 shows the differences between the reality and the protection scenarios (isolating the effect of the PFPTs), as detailed in Fig.S5 and Fig.S6. We observe that the PFPTs lead to moderate reductions in peak water depths across much of the inundated zone, of around 0.1-0.3m, with the biggest differences being in the peripheral areas, and in the central stream (Fig5A). Velocity reductions are spatially heterogeneous but pronounced where flow paths concentrate (Fig5B). Yellow to orange zones (0.2-0.8 m/s reductions) follow main overland flow corridors, while even bigger reductions (1.0-1.6 m/s, red–pink) are observed in the main stream's flooding, and the rest of the broad flat areas exhibit minor reductions (0-0.2 m/s, pale yellow). Such reductions, especially to the west part, can significantly reduce infrastructure damages.

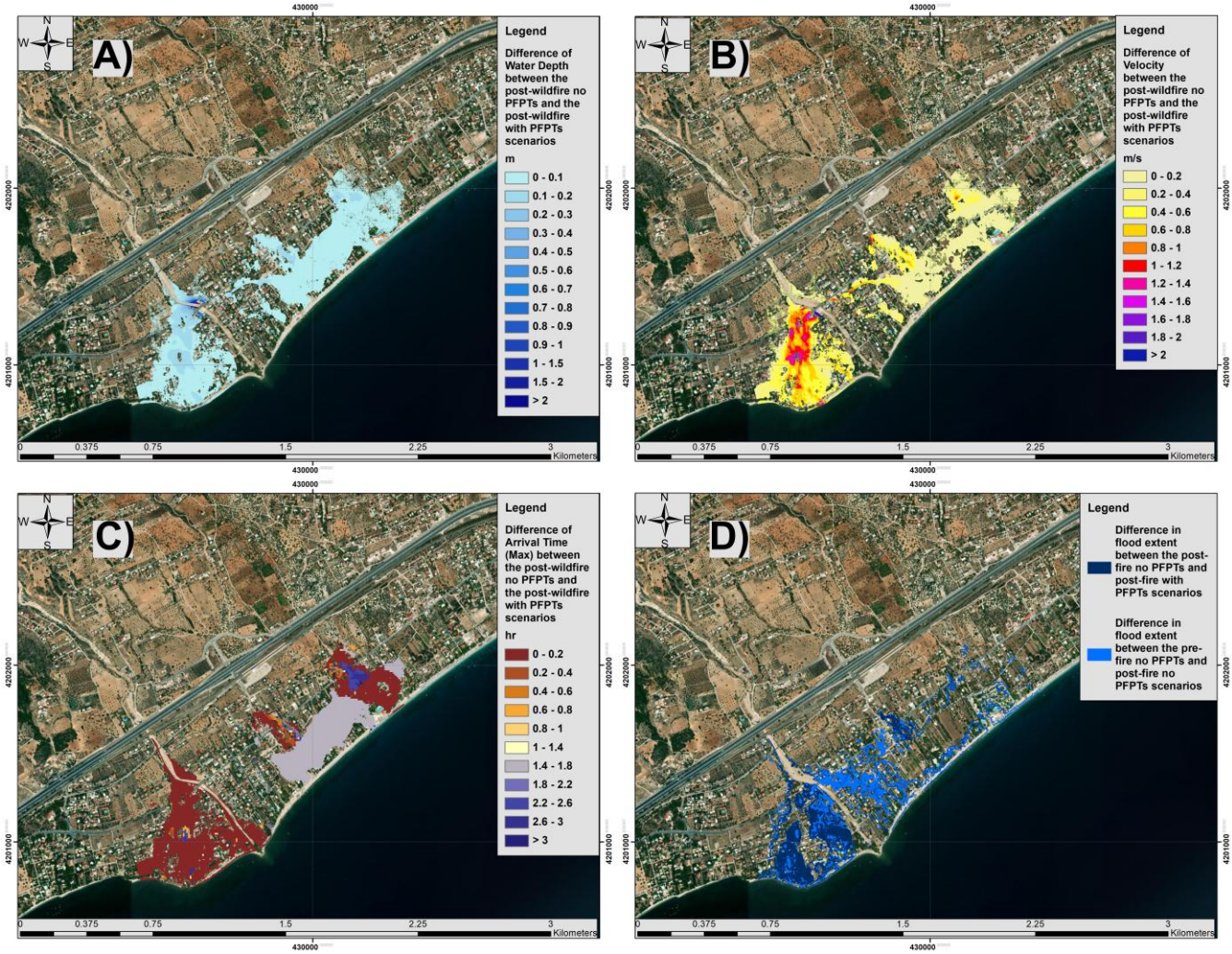

Figure 5: Assessment of the effect of the PFPTs on: A) Water depth, B) water velocity, C) Flood maximum arrival time, D) water extent. These are presented as the differences between the Post-wildfire No PFTs and Post-wildfire With PFPTs, while for the floodwater extent (D) we compare all scenarios. Base-map source: © Google Earth

The PFPTs introduce meaningful delays in flood wave arrival, as seen in the arrival-time difference map (Fig5C). Peripheral urban areas and floodplain margins experience minimal delays (0-0.4 h, brown–light orange), while central zones downstream of barrier clusters show delays of 1.0-2.2 h (light purple to deep blue). The central part of the city, which appears to be the most flood-prone, had the largest delays due to PFPTs, and this is crucial for emergency response, evacuation, traffic management, and individual protection measures. Moreover, elongated travel times reduce flood peaks, lessen hydraulic loads on downstream structures, and allow more water to infiltrate or be retained, showcasing PFPTs' role in temporal flood risk mitigation.

Regarding the flood extent, the dark blue areas would have been inundated without PFPTs but remain dry when they're in place. The blue shading shows the additional flood extent caused by the wildfire (post-wildfire with PFPTs vs. pre-wildfire without PFPTs), underscoring how burn-induced changes expand inundation inland. This joint comparison illustrates that while the post-wildfire landscape is inherently more flood-prone, strategically placed PFPTs can reclaim substantial areas from inundation.

3.4 Cost of protection and flood damage direct costs

The estimation of the cost of the recommended PFPTs considers the typical expenses for materials (wood), transportation, and construction (installation), in values of €2023, according to the official Greek techno-economic specifications (Table S4). Based on these estimations, the costs for the PFPTs designed for the Kineta catchment would be 4.87€ per meter of LEBs installed, and 49.25 €/m^2 of wooden check dams. The spatial model for the proposed PFPTs (Fig.S3) resulted in 636,049 m of LEBs and 2065 wooden check dams (of an average installed area of 3.5 m^2). Therefore, their total cost would be:

- 4.87€/m · 636,049 m of LEBs installed = €3.1mill, plus
- 49.25 €/m^2 · 2065 per wooden check dams ·3.5 m^2 each = 355,954€,

Which, in total, sums to €3.45 mill. The final PFPTs cost, including the overhead and contractor's profit margin and the VAT, is €5,05 mil.

The total estimated flood damage cost considered residential house properties, commercial buildings (namely hotels in the area), private vehicles, agricultural fields, the closure of the Athens-Corinth highway for an entire working day, and reported infrastructure damages to roads, streams, land, and drainage. A semi-automated AI image segmentation and human counting approach was applied to count the affected elements, and we assigned monetary values to them based on insurance data. For the highway closure due to the flood, a general estimation model for such economic losses was applied (see Eq.S2 in the SI). This applied to all scenarios, given the severity of the flood, with the water reaching up to the road in all simulations. The infrastructure cost was adjusted based on the flooded area of each scenario.

The resulting total cost of €25.2mill was cross-checked and validated over the estimates of the West Attica's Region Technical Works Observatory on the total repair costs (which was reported to be €21.6mill) (West Attica Region, 2021). The total estimated cost, considering all these components is €25.2mill.

The results of the PFPTs costs and flood damages are summarized as follows:

- **Pre-wildfire, No PFPTs:** Reduced count of residential homes, commercial buildings (hotels), private vehicles, and agricultural fields affected compared to the "reality" scenario; Same cost for the same highway closure; Reduced infrastructure cost based on the reduced flooded area, compared to the "reality" scenario. Cost of PFPTs = 0€. Flood damage cost = €19.1mill. The difference in the flood damage cost is 6,136,996€ (or 24.33% of the real event's damage), which is purely attributed to the wildfire.
- **Post-wildfire, No PFPTs:** The exact affected number of residential homes, commercial buildings (hotels), private vehicles, and agricultural fields; Actual cost for the Athens-Corinth highway closure; Actual infrastructure cost. Cost

of PFPTs = 0€. Flood damage cost = €25.2mill. This represents the real case, which highlights the extensive financial burden on local authorities and communities, underscoring the need for effective flood management and mitigation strategies to reduce long-term economic impacts.

- **Post-wildfire, With PFPTs:** Reduced count of residential homes, commercial buildings (hotels), private vehicles, and agricultural fields; Same cost for the same highway closure; Reduced infrastructure cost based on the reduced flooded area. Cost of PFPTs = €5.05mill, Flood damage cost = €18.9mill. The difference in the flood damage cost is €6.4mill. This indicates that the PFPTs could have reduced the actual real case's flood damage costs by 25.3%, completely offsetting the wildfire's impact.

4 Discussion

4.1 Modelling post-wildfire floods and PFPTs

The representation of the post-wildfire flood event, considering a combination of methods (meteorologic model, RS, hydraulic-hydrodynamic, and spatial PFPTs-design model) is a challenging and interdisciplinary modelling task. With this combined modelling approach, on the one hand, we provide a framework for similar analyses, as all models are freely available and can be used in combination (soft-linked) to represent other post-wildfire flood events. On the other hand, this approach led to accurate representation that enables building on the findings (flood inundation maps) to consider protection measures and enhance resilience. Also, the modelling of the PFPTs within HEC-RAS is a novel application. An interesting set of findings here is the wildfire's and the PFPTs' effects on flooding. The effect of the wildfire on the flood extent is 24.1% (difference of the pre- and post-wildfire scenarios), which is not negligible for a small town. Regarding the effectiveness of the PFPTs, if the recommended measures were in place, 24.8% of the flooding would have been avoided, while most of the floodwaters would have been delayed, coming with reduced velocities and depths.

4.2 Exploring the effect of PFPTs

The analysis for the application of the most suitable PFPTs, their mapping, and cost-effectiveness is also a challenging task, as the literature on PFPTs is limited. To the best of our knowledge, this is the first attempt to model PFPTs based on spatially modelled physical characteristics and case-study-specific technical guidelines, along with a detailed assessment of their cost-effectiveness for flood mitigation. This approach illustrates how the PFPTs can be followed to other study areas, similarly, and give at least a preliminary picture/estimation of the potential post-wildfire measures. As mentioned, their effectiveness is significant, completely offsetting the wildfire's impact on flooding. Especially if we consider the significance of the downstream residential area, and take into account the overall effects in water extent, depth, velocity, and arrival times, as well as the relatively low costs, there is no doubt on the PFPTs' value. In addition to reducing flood extent, the PFPT scenario also resulted in lower flow depths and velocities (Fig. 5A–B), with velocity reductions exceeding 1.0 m/s in parts of the main

channel. These reductions are directly linked to flood hazard intensity and damage severity, further supporting the protective value of the proposed measures.

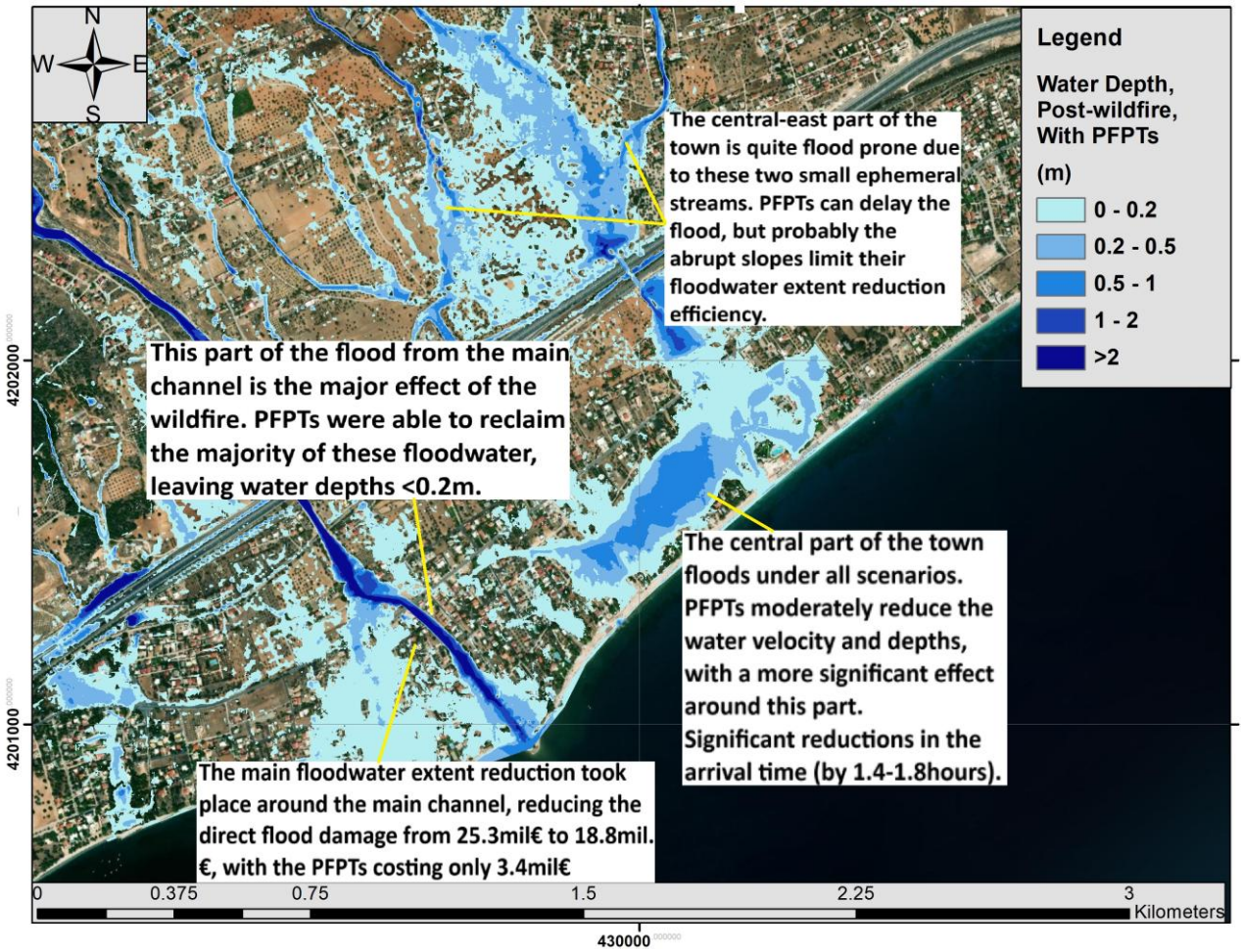

Figure 6: Summarizing the main findings on the effect of PFPTs, over the Post-wildfire With PFPTs scenario. Base-map source: © Google Earth.

To our knowledge there is no other study exploring all these flood- and PFPTs-related effects with hydraulic modelling based on a real post-fire event. In order to validate or cross-check our findings with the broader literature, we also reviewed field based studies from the Mediterranean area. Indeed, the results are consistent, demonstrating the effectiveness of small-scale interventions in reducing post-fire runoff and sediment yield. Margiorou et al. (2022) showed that wooden check dams significantly reduced sediment discharge in burned suburban catchments, while Kastridis et al. (2022) emphasized their cost-efficiency when combined with other erosion control measures. Furthermore, Theofanidis et al. (2025) highlighted that the timing of PFPT implementation is crucial, early post-fire construction enhances sediment interception and reduces downstream

impacts. The convergence of our model-based findings with field evidence underscores the mitigation role of PFPTs when rapidly deployed and appropriately located within affected catchments.

Overall, as Fig.6 summarizes, the PFPTs are particularly effective along the main stream, where well-established flowpaths and gentle slopes allow LEBs and WCD to intercept and attenuate floodwaters over long reaches. This configuration not only reduces peak velocities but also meaningfully delays water arrival times, offering valuable lead-time for downstream communities. In contrast, PFPTs prove less efficient in the smaller Intermittent Rivers and Ephemeral Streams (IRES) in the northeast part of the catchment with steeper, more abrupt slopes. These were responsible for the majority of the flooding, indicating the need to map IRES, as they are not mapped in Greece (Pastor et al., 2022), and usually not considered in flood protection plans, however, as proved, these can cause severe damages, under all scenarios. Yet even here PFPTs can substantially slow the initial flood buildup, providing critical flood delay in the town centre.

It is worth noting that the storm of November 2019 was a severe phenomenon, that would have caused flooding under all scenarios, underscoring the vulnerability of the area, and the need of perhaps even more strict flood protection works. The PFPTs largely mitigate the wildfire's hydrological impact, rather than the flood event itself: even under pre-wildfire conditions, this storm was severe enough to inundate much of the floodplain. Thus, additional and more robust flood defences remain essential for events of this magnitude.

4.3 Economic assessment

The cost of the PFPTs, the flood damage direct cost, and ultimately their comparison, were insightful for the cost-effectiveness of protection investments. The cost of the examined PFPTs resulted to €5.05mill, while the direct flood damage cost was estimated to €25.2mill (around 5 times higher). This indicates a considerable difference, with the cost of the measures aiming to the flood damage mitigation (PFPTs) being just the 20% of (only) the direct flood damage costs. This is a 'lesson in preparedness', highlighting that investing in mitigation works can help reducing much larger hazard-induced damages.

At this point, the limitations should be mentioned. Due to unavailable data, we did not consider certain components of the flood damage cost – in particular, those beyond the direct costs: The economic impact of business interruption caused by the flood (this includes lost revenue, additional expenses incurred due to downtime, and potential long-term impacts on business operations) has not been considered. Moreover, the health impacts of the flood, including medical expenses, emergency response costs, and potential long-term health effects were not taken into account in the flood damage cost estimations. Other environmental damages such as pollution, habitat destruction, and cleanup costs, were not considered. Finally, the community and social costs were also ignored (including displacement of residents, loss of community services, and psychological effects). So, our flood damage cost estimates are quite conservative (just the direct costs), and in reality, they are way higher – significantly more than five times the investment in post-wildfire flood protection. Moreover, the flood damage estimation was primarily based on the flooded area. In the protection scenario (Post-wildfire, With PFPTs), we observed that even if there was floodwater in some parts, the depth was lower than 20-10cm, and the velocity was also negligible, indicating that in reality the damage cost might have been less than €18.9mill. At the same time, the PFPT measures proposed for the case of Kineta

are also conservative (i.e., a dense network of LEBs and wooden check-dams was proposed), but other approaches might consider less PFPTs, significantly lowering their costs. Having a 'low-end' estimate of flood damage cost, and a 'high-end' estimate of the PFPTs' costs, and still proving their significant difference, highlights even more the fact that 'precaution' seems to be a wiser decision than 'cure'.

5 Conclusions

The findings of this modelling study, beyond the general framework provided for the integrated analysis of similar phenomena, show the importance of investing in the flood resilience of burned sites. This study showed that the PFPTs would have been able to reduce a substantial floodwater amount, somewhat larger than the entire flood that was due to the wildfire. Of course, this does not mean that if the PFPTs had been in place after the wildfire, the flood would have been totally avoided. In other words, the investment of approximately €5.05mill would not have been enough to avoid the €25.2mill flood damage cost. However, the flood would have been mitigated, saving at least €7mill from the damages. Again, this estimate is quite conservative, as explained in the discussion section; therefore, we believe that the investment in preparedness is definitely worthwhile. For now, our findings can provide food for thought and serve as a lesson in preparedness, indicating that post-wildfire flood protection can be a cost-effective decision, relatively inexpensive, and can be achieved at local scales (e.g., at the municipality scale) with local means.

A follow-up question from this research is on the need to map the IRES, and those like the one in Kineta that have abrupt slopes, to consider enhanced protection measures. Another follow-up question is, although the studied storm was indeed extreme and caused a flood under all scenarios, why are these protection measures not applied to mitigate it? One possible explanation is limited awareness among decision-makers, combined with weak communication and possibly lack of trust between authorities and experts who hold relevant knowledge. Another explanation could be that decision-makers consider PFPTs as an expensive objective compared to flood damage costs, which will not likely grab headlines (in contrast to news reporting a big fire or flood) (Nature Sustainability, 2023). Following the wildfires in Kineta, Greek newspapers argued that a significant investment in preventive measures is necessary to address future flood risks, noting that even after the flood, there was still no protection work in place (Chaini, 2019). Often, flood damage compensation is not being paid in Greece, and restoration works are being significantly delayed. This also occurred in Kineta, where the latest reports on the case indicate that the compensation for the affected households was still pending (Papadopoulou, 2025). Therefore, if there is a tendency to dismiss flood damage compensation, then the application of PFPTs seems indeed like an unnecessary and undesirable expense. At the end of 2024, after extended protests, the case of Kineta was brought to court, as no PFPTs were in place, nor compensations were granted. The primary defendant is the Former Regional Governor of Attica, and the case is underway (Protothema, 2024).

Further science-to-policy bridges and collaboration can significantly improve our understanding of complex hazards, such as post-wildfire floods, an often-overlooked topic, and assess the potential of PFPTs, while highlighting the need for timely resilience-building and preparedness as a necessary step, rather than inaction.

Data availability: All data can be made available from the corresponding author upon request.

Author contributions: Conceptualization was carried out by G.P. and A.A.. Methodology was contributed by all authors. Software development was performed by G.P., A.A., M.B., V.M., G.V., and N.N.. Data analysis was carried out by G.P., A.A., M.B., N.N., V.M., G.V., and A.P.. Writing—original draft preparation was undertaken by G.P. and A.A., while writing—review and editing involved all authors.

Competing interests: The authors declare that they have no conflict of interest.

Acknowledgements: P.K. acknowledges funding from the European Research Council (ERC) under the ERC Synergy Grant Water-Futures grant agreement ID 951424.

References

Alamanos, A.: Exploring the Impact of Future Land Uses on Flood Risks and Ecosystem Services, With Limited Data: Coupling a Cellular Automata Markov (CAM) Model, With Hydraulic and Spatial Valuation Models, Qeios, https://doi.org/10.32388/JJWWBD, 2024.

Alamanos, A., Papaioannou, G., Varlas, G., Markogianni, V., Plataniotis, A., Papadopoulos, A., Dimitriou, E., and Koundouri, P.: Designing Post-Fire Flood Protection Techniques for a Real Event in Central Greece, Prevention and Treatment of Natural Disasters, 3, 2024a.

Alamanos, A., Papaioannou, G., Varlas, G., Markogianni, V., Papadopoulos, A., and Dimitriou, E.: Representation of a Post-Fire Flash-Flood Event Combining Meteorological Simulations, Remote Sensing, and Hydraulic Modeling, Land, 13, 47, https://doi.org/10.3390/land13010047, 2024b.

Nature Sustainability: Time to recover, Nat Sustain, 6, 1027–1027, https://doi.org/10.1038/s41893-023-01228-z, 2023.

Basheer, M. and Oommen, T.: PyLandslide: A Python tool for landslide susceptibility mapping and uncertainty analysis, Environmental Modelling & Software, 177, 106055, https://doi.org/10.1016/j.envsoft.2024.106055, 2024.

Brémond, P., Grelot, F., and Agenais, A.-L.: Review Article: Economic evaluation of flood damage to agriculture – review and analysis of existing methods, Natural Hazards and Earth System Sciences, 13, 2493–2512, https://doi.org/10.5194/nhess-13-2493-2013, 2013.

Brogan, D. J., MacDonald, L. H., Nelson, P. A., and Morgan, J. A.: Geomorphic complexity and sensitivity in channels to fire and floods in mountain catchments, Geomorphology, 337, 53–68, https://doi.org/10.1016/j.geomorph.2019.03.031, 2019a.

Brogan, D. J., Nelson, P. A., and MacDonald, L. H.: Spatial and temporal patterns of sediment storage and erosion following a wildfire and extreme flood, Earth Surface Dynamics, 7, 563–590, https://doi.org/10.5194/esurf-7-563-2019, 2019b.

Chaini, A.: No flood protection works in Kineta: the causes of the disaster, Ecozen, 2019.

Chrysovergis, P., Chrysovergis, S., and Chrysovergis, T.: An Evaluation of Post-Wildfire Erosional and Flooding Damage in Southern California, 116–128, https://doi.org/10.1061/9780784483688.012, 2021.

Cos, J., Doblas-Reyes, F., Jury, M., Marcos, R., Bretonnière, P.-A., and Samsó, M.: The Mediterranean climate change hotspot in the CMIP5 and CMIP6 projections, Earth System Dynamics, 13, 321–340, https://doi.org/10.5194/esd-13-321-2022, 2022.

Ebel, B. A. and Martin, D. A.: Meta-analysis of field-saturated hydraulic conductivity recovery following wildland fire: Applications for hydrologic model parameterization and resilience assessment, Hydrological Processes, 31, 3682–3696, https://doi.org/10.1002/hyp.11288, 2017.

Girona-García, A., Vieira, D. C. S., Silva, J., Fernández, C., Robichaud, P. R., and Keizer, J. J.: Effectiveness of post-fire soil erosion mitigation treatments: A systematic review and meta-analysis, Earth-Science Reviews, 217, 103611, https://doi.org/10.1016/j.earscirev.2021.103611, 2021.

Girona-García, A., Cretella, C., Fernández, C., Robichaud, P. R., Vieira, D. C. S., and Keizer, J. J.: How much does it cost to mitigate soil erosion after wildfires?, J Environ Manage, 334, 117478, https://doi.org/10.1016/j.jenvman.2023.117478, 2023.

Godara, N., Bruland, O., and Alfredsen, K.: Simulation of flash flood peaks in a small and steep catchment using rain-on-grid technique, Journal of Flood Risk Management, 16, e12898, https://doi.org/10.1111/jfr3.12898, 2023.

Greek Ministry of Environment and Energy: Study on soil-erosion and flood protection works at the burnt area of the Avantas catchment and surounding settlements. Decentralized Administration of Macedonia and Thrace. (in Greek), 2023.

Grell, G. A. and Freitas, S. R.: A scale and aerosol aware stochastic convective parameterization for weather and air quality modeling, Atmospheric Chemistry and Physics, 14, 5233–5250, https://doi.org/10.5194/acp-14-5233-2014, 2014.

Hasan, M. M., Burian, S., and Barber, M. E.: Determining The Impacts Of Wildfires On Peak Flood Flows In High Mountain Watersheds, International Journal of Environmental Impacts, 3(2020), 12, https://doi.org/10.2495/EI-V3-N4-339-351, 2020.

Havel, A., Tasdighi, A., and Arabi, M.: Assessing the hydrologic response to wildfires in mountainous regions, Hydrology and Earth System Sciences, 22, 2527–2550, https://doi.org/10.5194/hess-22-2527-2018, 2018.

Hong, S.-Y., Dudhia, J., and Chen, S.-H.: A Revised Approach to Ice Microphysical Processes for the Bulk Parameterization of Clouds and Precipitation, Monthly Weather Review, 132, 103–120, https://doi.org/10.1175/1520-0493(2004)132<0103:ARATIM>2.0.CO;2, 2004.

Hydrologic Engineering Center (HEC): River Analysis Systems - HEC-RAS (Version 6.3.1). U.S. Army Corps of Engineers., 2022.

Iacono, M. J., Delamere, J. S., Mlawer, E. J., Shephard, M. W., Clough, S. A., and Collins, W. D.: Radiative forcing by long-lived greenhouse gases: Calculations with the AER radiative transfer models, Journal of Geophysical Research: Atmospheres, 113, https://doi.org/10.1029/2008JD009944, 2008.

Kastridis, A. and Kamperidou, V.: Evaluation of the post-fire erosion and flood control works in the area of Cassandra (Chalkidiki, North Greece), J. For. Res., 26, 209–217, https://doi.org/10.1007/s11676-014-0005-9, 2015.

Kastridis, A., Margiorou, S., & Sapountzis, M. (2022). Check-Dams and Silt Fences: Cost-Effective Methods to Monitor Soil Erosion under Various Disturbances in Forest Ecosystems. Land, 11(12), 2129. https://doi.org/10.3390/land11122129

Kirillov, A., Mintun, E., Ravi, N., Mao, H., Rolland, C., Gustafson, L., Xiao, T., Whitehead, S., Berg, A. C., Lo, W.-Y., Dollár, P., and Girshick, R.: Segment Anything, https://doi.org/10.48550/arXiv.2304.02643, April 5th 2023.

Koudoumakis, P., Keramitsoglou, K., Protopapas, A. L., and Dokas, I.: A general method for multi–hazard intensity assessment for cultural resources: Implementation in the region of Eastern Macedonia and Thrace, Greece, International Journal of Disaster Risk Reduction, 100, 104197, https://doi.org/10.1016/j.ijdrr.2023.104197, 2024.

Kourgialas, N. N.: A critical review of water resources in Greece: The key role of agricultural adaptation to climate-water effects, Science of The Total Environment, 775, 145857, https://doi.org/10.1016/j.scitotenv.2021.145857, 2021.

Lekkas, E., Spyrou, N., Filis, C., Diakakis, M., Vassilakis, E., Katsetsiadou, A., Milios, D., Arianoutsou, M., Faragitakis, G., Christopoulou, A., and Antoniou, V.: The November 25th, 2019 Kineta (Western Attica) Flood., Athens, Greece, 2019.

Margiorou, Stella, Aristeidis Kastridis, and Marios Sapountzis. 2022. "Pre/Post-Fire Soil Erosion and Evaluation of Check-Dams Effectiveness in Mediterranean Suburban Catchments Based on Field Measurements and Modeling" Land 11, no. 10: 1705. https://doi.org/10.3390/land11101705

Merz, B., Kreibich, H., Thieken, A., and Schmidtke, R.: Estimation uncertainty of direct monetary flood damage to buildings, Natural Hazards and Earth System Sciences, 4, 153–163, https://doi.org/10.5194/nhess-4-153-2004, 2004.

Meteosearch | Weather Data Portal: https://meteosearch.meteo.gr/, last access: April 13th 2024.

Mitsopoulos, G., Diakakis, M., Panagiotatou, E., Sant, V., Bloutsos, A., Lekkas, E., Baltas, E., and Stamou, A. I.: 'How would an extreme flood have behaved if flood protection works were built?' the case of the disastrous flash flood of November 2017 in Mandra, Attica, Greece, Urban Water Journal, 19, 911–921, https://doi.org/10.1080/1573062X.2022.2103002, 2022.

Nandam, V. and Patel, P. L.: A framework to assess suitability of global digital elevation models for hydrodynamic modelling in data scarce regions, Journal of Hydrology, 630, 130654, https://doi.org/10.1016/j.jhydrol.2024.130654, 2024.

Napper, C.: Burned Area Emergency Response Treatments (BAER) Catalog; US Forest Service: Washington, DC, USA; San Dimas Technology and Development Center: San Dimas, CA, USA., 2006.

NCMA (2021). National Cadastre and Mapping Agency S.A. (NCMA).

Papadopoulou, A. (2025). Shocking testimonies about the flood in Kineta in 2019: https://www.efsyn.gr/ellada/dikaiosyni/456701_sygklonistikes-martyries-gia-tin-plimmyra-stin-kineta-2019#goog_rewarded, last access: March 25th 2025.

Papaioannou, G., Vasiliades, L., Loukas, A., Alamanos, A., Efstratiadis, A., Koukouvinos, A., Tsoukalas, I., and Kossieris, P.: A Flood Inundation Modeling Approach for Urban and Rural Areas in Lake and Large-Scale River Basins, Water, 13, 1264, https://doi.org/10.3390/w13091264, 2021.

Papaioannou, G., Alamanos, A., and Maris, F.: Evaluating Post-Fire Erosion and Flood Protection Techniques: A Narrative Review of Applications, GeoHazards, 4, 380–405, https://doi.org/10.3390/geohazards4040022, 2023.

576 Pastor, A. V., Tzoraki, O., Bruno, D., Kaletová, T., Mendoza-Lera, C., Alamanos, A., Brummer, M., Datry, T., De Girolamo,
577 A. M., Jakubínský, J., Logar, I., Loures, L., Ilhéu, M., Koundouri, P., Nunes, J. P., Quintas-Soriano, C., Sykes, T., Truchy, A.,
578 Tsani, S., and Jorda-Capdevila, D.: Rethinking ecosystem service indicators for their application to intermittent rivers,
579 Ecological Indicators, 137, 108693, https://doi.org/10.1016/j.ecolind.2022.108693, 2022.

580 Posner, A. J. and Georgakakos, K. P.: Quantifying the impact of community-scale flood mitigation, International Journal of
581 Disaster Risk Reduction, 24, 189–208, https://doi.org/10.1016/j.ijdrr.2017.06.001, 2017.

582 Protothema: Storm "Girionis": How Kineta was burned - Visual inspection in the area, ProtoThema, 25th November, 2019.

583 Protothema: The trial for the Kineta flood begins this autumn. Patoulis to be the first defendant., Athens, Greece, 2024.

584 Robinne, F.-N., Hallema, D. W., Bladon, K. D., and Buttle, J. M.: Wildfire impacts on hydrologic ecosystem services in North
585 American high-latitude forests: A scoping review, Journal of Hydrology, 581, 124360,
586 https://doi.org/10.1016/j.jhydrol.2019.124360, 2020.

587 Tewari, M., Boulder, C., Chen, F., Wang, W., Dudhia, J., LeMone, M., Mitchell, K., Ek, M., Gayno, G., Wegiel, J., and
588 Cuenca, R.: Implementation and verification of the unified Noah land surface model in the WRF model, in: 20th Conference
589 on Weather Analysis and Forecasting/16th Conference on Numerical Weather Prediction, 20th Conference on Weather
590 Analysis and Forecasting/16th Conference on Numerical Weather Prediction, 2004.

591 Theochari, A.-P. and Baltas, E.: Holistic hydrological approach to the fire event on August 2021 in Evia, Greece, Euro-Mediterr
592 J Environ Integr, 7, 287–298, https://doi.org/10.1007/s41207-022-00304-8, 2022.

593 Theofanidis, A., Kastridis, A., & Sapountzis, M. (2025). Effectiveness of Torrential Erosion Control Structures (Check Dams)
594 Under Post-Fire Conditions—The Importance of Immediate Construction. Land, 14(3), 629.
595 https://doi.org/10.3390/land14030629

596 Thieken, A. H., Ackermann, V., Elmer, F., Kreibich, H., Kuhlmann, B., Kunert, U., Maiwald, H., Merz, B., Müller, M., Piroth,
597 K., Schwarz, J., Schwarze, R., Seifert, I., and Seifert, J.: Methods for the evaluation of direct and indirect flood losses, RIMAX
598 Contributions at the 4th International Symposium on Flood Defence (ISFD4), 2009.

599 Varlas, G., Papadopoulos, A., Papaioannou, G., Markogianni, V., Alamanos, A., and Dimitriou, E.: Integrating Ensemble
600 Weather Predictions in a Hydrologic-Hydraulic Modelling System for Fine-Resolution Flood Forecasting: The Case of Skala
601 Bridge at Evrotas River, Greece, Atmosphere, 15, 120, https://doi.org/10.3390/atmos15010120, 2024.

602 Wang, J., Stern, M. A., King, V. M., Alpers, C. N., Quinn, N. W. T., Flint, A. L., and Flint, L. E.: PFHydro: A New Watershed-
603 Scale Model for Post-Fire Runoff Simulation, Environmental Modelling & Software, 123, 104555,
604 https://doi.org/10.1016/j.envsoft.2019.104555, 2020.

605 West Attica Region: Restoration of damages for the local community of Kineta. West Attica's Technical Works Observatory.,
606 2021.

607 Wu, J., Nunes, J. P., Baartman, J. E. M., and Faúndez Urbina, C. A.: Testing the impacts of wildfire on hydrological and
608 sediment response using the OpenLISEM model. Part 1: Calibration and evaluation for a burned Mediterranean forest
609 catchment, CATENA, 207, 105658, https://doi.org/10.1016/j.catena.2021.105658, 2021.

610 Zabret, K., Hozjan, U., Kryžanowsky, A., Brilly, M., and Vidmar, A.: Development of model for the estimation of direct flood
611 damage including the movable property, Journal of Flood Risk Management, 11, S527–S540,
612 https://doi.org/10.1111/jfr3.12255, 2018.

Zotou, I., Karamvasis, K., Karathanassi, V., and Tsihrintzis, V. A.: Potential of Two SAR-Based Flood Mapping Approaches in Supporting an Integrated 1D/2D HEC-RAS Model, Water, 14, 4020, https://doi.org/10.3390/w14244020, 2022.